MDPI

Article

Life Cycle Assessment of a Lithium-Ion Battery Pack Unit Made of Cylindrical Cells

Morena Falcone [1,*], Nicolò Federico Quattromini [2,*], Claudio Rossi [2,*] and Beatrice Pulvirenti [1,*]

1   Department of Industrial Engineering, Alma Mater Studiorum Università di Bologna, Viale Risorgimento, 2, 40136 Bologna, Italy
2   Department of Electrical, Electronic and Information Engineering "Guglielmo Marconi", Alma Mater Studiorum Università di Bologna, Viale Risorgimento, 2, 40136 Bologna, Italy
*   Correspondence: morena.falcone@unibo.it (M.F.); nicolo.quattromini@studio.unibo.it (N.F.Q.); claudio.rossi@unibo.it (C.R.); beatrice.pulvirenti@unibo.it (B.P.)

Abstract: Saving energy is a fundamental topic considering the growing energy requirements with respect to energy availability. Many studies have been devoted to this question, and life cycle assessment (LCA) is increasingly acquiring importance in several fields as an effective way to evaluate the energy demand and the emissions associated with products' life cycles. In this work, an LCA analysis of an existent lithium-ion battery pack (BP) unit is presented with the aim to increase awareness about its consumption and offering alternative production solutions that are less energy intensive. Exploiting the literature data about cradle-to-grave and cradle-to-gate investigations, and after establishing reasonable approximations, the main BP sub-elements were considered for this study, such as the plastic cells support, the Li-ion cells brick, the PCBs for a battery management system (BMS), the liquid-based battery thermal management system (BTMS) and the BP container. For each of these components, the impacts of the extraction, processing, assembly, and transportation of raw materials are estimated and the partial and total values of the energy demand (ED) and global warming potential (GWP) are determined. The final interpretation of the results allows one to understand the important role played by LCA evaluations and presents other possible ways of reducing the energy consumption and CO_2 emissions.

Keywords: life cycle assessment; energy demand; global warming potential; cradle-to-gate; battery pack; lithium-ion; energy saving

1. Introduction

In a society where the energy demand is constantly growing hand in hand with technological development and, at the same time, awareness of environmental issues is rising, studies of life cycle assessment (LCA) have become fundamental. Before 2015, when the EU Circular Economy Action Plan had not yet come into play [1], the LCA was already a discussion topic but mainly in research environments. The outdated and most common way of approaching goods production was mainly focused on performances and costs in "linear life thinking", which caused dramatic results in terms of raw material usage. The United Nations Environment Programme (UNEP) stated that, in the last 40 years, raw material consumption tripled, going from 27 billion tons in 1970 to 98 billion tons in 2018 [2]. In the last decade, the LCA has generated more and more interest not only in the academic world but also among industry stakeholders who have begun to change their mindset, switching to the new "circular life thinking" or life cycle thinking (LCT) [3]. Both private realities (industries, companies) and public ones (governments) have started to embrace green economy principles, establishing and regulating business models so that both materials and products can keep their highest value throughout their whole life cycles [4,5]. This new way of thinking about the product impact does not only consider its disposal stages [6] but also all the production phases from the extraction of raw materials

to the manufacturing processes, including the use of energy and water [7,8], wastes and transportation emissions [9]. Finally, the disposal of the product is investigated, taking into account the possibility of recycling all or part of it [10,11]. This last consideration is the key-point that allows distinguishing two different approaches to the product impact: the cradle-to-grave (CTG) and the cradle-to-cradle (CTC).

The CTG approach dates from the 1990s [6] and takes into account the whole life cycle of a product up to the disposal stage. It has increased producers' awareness of the real consumption related to their production, teaching the LCT and motivating them not to waste resources. Regarding the CTC approach, it does not consider the analysis impact of a real final disposal phase as what is considered waste in CTG studies is "food" for CTC ones. It was in 2002 that the definition of CTC was given by the chemist Michael Braungart and the architect William McDonough: drawing a parallel with nature where "the waste of one system becomes food for another" [12], they suggested a product impact approach where the products which arrived at the end of their lives would have become a sort of raw material to produce something of equal or even better quality. This innovative LCT implied recycling processes which, in recent decades, have been significantly developed and improved in every field. The International Organization for Standardization (ISO) includes widely recognized procedures to conduct valid and extensive LCA studies [13]. In particular, ISO 14040 and ISO 14044 represent the basis of the International Reference Life Cycle Data System (ILCD), a technical guideline to carry on accurate LCAs considering product-specific criteria [3].

To complete a detailed and useful LCA, ISO 14040 and ISO 14044 suggest to proceed by following four different phases which are often dependent on each other. Nevertheless, none of these stages should be considered as concluded until the entire study is complete. The aforementioned stages are the following: goal and scope; life cycle inventory (LCI); life cycle impact assessment (LCIA); and interpretation. During the goal and scope stage, the intended application and audience, the reason for the study and whether the results will be used in a comparative dissertation intended for public release must be defined. This is a fundamental preliminary phase which saves time during the following ones by focusing the attention on the real core of the investigation. The LCI is the data collecting phase resulting from an input and output analysis and quantification: this is the moment when a real inventory is compiled [14] considering raw materials, energy and water requirements, atmospheric emissions, resource usage and all the other flows involved in a product or process life cycle. Flow charts, such as the Sankey diagram, are very helpful during this phase [15]. Knowing the methods to extract or machine the materials, it is possible to work on the impact assessment. First, it is necessary to classify the kind of impact associated with the considered material (climate change, ozone depletion, or toxicity related to anthropogenic activity). Then, all the inventory items (flows) have to be characterized: this means that every flow related to a certain impact has to be classified under a common unit of comparison [13]. For instance, considering the global warming potential (GWP) as the impact, the unit is the equivalent CO_2 weight which has to be assigned to all the items in the inventory. This procedure is usually performed with the help of databases. Finally, there is the interpretation of the collected data: the LCI and the LCIA are checked, evaluated and all the issues coming from the investigation of these two previous phases are identified and faced by choosing among a broad repertoire of methodological alternatives [16]. A series of limitations and recommendations represents the final result of the interpretation phase.

Nowadays, LCA studies focus on extremely varied fields of services and products, such as packaging [17], tourism [18], textile industry [19,20], food processes [21–24], drink consumption [25,26], electronics [27], and materials [28]. Transportation is another huge sector in which LCA analysis is applied [29], and particularly when considering the issue of sustainable urban and commercial development, many studies have investigated the benefits brought by the electrification of the public means compared to the impacts of more ordinary thermal-engine-powered vehicles [30–32]; on the other hand, other studies have analyzed the positive environmental and economic impacts resulting from a ships

electrification campaign, considering factors, such as the kind of fuel/propulsion, the chemistry of the BPs, and the average cruise speed [33–36]. A great deal of effort is also focused on the automotive field, studying the effects of car lightening [37], the benefits of using recycled natural materials [38], and, when it talks about green mobility [39–41], the attention is often focused on the Li-ion BP. Several researches deal with the environmental impact of a whole electric vehicle (EV) BP [42], other studies focus on the constituent materials [43] or components [44–46].

In this paper, LCA literature results are used to carry on a cradle-to-gate analysis regarding the *LiBER* [47] BP based on the modular integration of lithium-ion cylindrical cells. This prototype is based on an international patent [48], whose main innovations are the modularity of the system, the thermal control of each cell in order to prevent thermal runaway events and some novel processes for the assembling of the cells and the bricks which avoid the use of wires. A custom-made battery pack based on the concept of the LiBER group has been installed on *Emilia 4* [49], the solar car of the University of Bologna built by the sport association *Onda Solare*. *Emilia 4* is a 4-seats competitive vehicle, fully made of carbon fibers, whose main characteristics are: two rear in-wheel electric motors, 5 m^2 of monocrystalline silicon solar panels and a 32 kWh Li-ion battery pack. Several studies have already been devoted to design, environmental, mechanical, and electrical aspects related to *Onda Solare* solar cars [50–58]. Taking into account *Emilia 4*, the aim of this work is to deepen the knowledge regarding the environmental impact of its BP. This study deals with the raw materials extraction, their processing, the assembly of the components, and the products transportation. All these stages are evaluated in terms of energy demand (ED) and GWP impact. A final interpretation of the results proposes several energy saving solutions to lower the *ED* and *GWP* values.

2. Materials and Methods

Figure 1 shows the Li-ion battery (LIB) considered for this analysis, which is made of 2 modules, both of them composed of a stack of 15 bricks which, in turn, contains 48 cells each. Figure 2 shows a detailed view of the LiBER brick: the 48 cells are inserted into the slots of the support structure, which is made of acrylonitrile butadiene styrene (ABS).
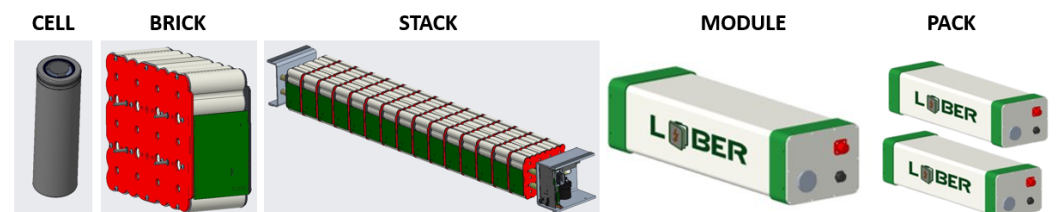

Figure 1. A scheme of the *LiBER* modular approach.

In the brick, as shown in Figure 2, the cells are separated from the ABS by means of thin aluminum liners, locked in the right position by two bus-bar plates and electrically connected to the positive and negative bus-bars by means of laser welded tabs. Additional holes in the support structure host the cooling piping. A printed circuit board called BMS-brick is installed on the side of each brick and it is used for the acquisition of the cells voltage and temperature. The bus-bars host the power connections which allow the direct connection in series of the bricks forming a stack of bricks. At the two ends, the stack is completed with electrical terminations, BMS control boards, and ancillaries. The module is formed by inserting the complete stack into a container made of composite material. The container is closed at the two sides with two metal plates to guarantee mechanical protection and to seal the modules. Finally, the two modules are connected either in series

or in parallel by using external power wiring to form the BP. The *LiBER* battery design for simple disassembling and reassembly operations, combined with a distributed State of Health (SOH) estimator, allows an easy reuse of the bricks in second life applications. This analysis regarding the LCA over a longer life time that includes disassembly, reassembly, and reuse will be addressed in a next work.
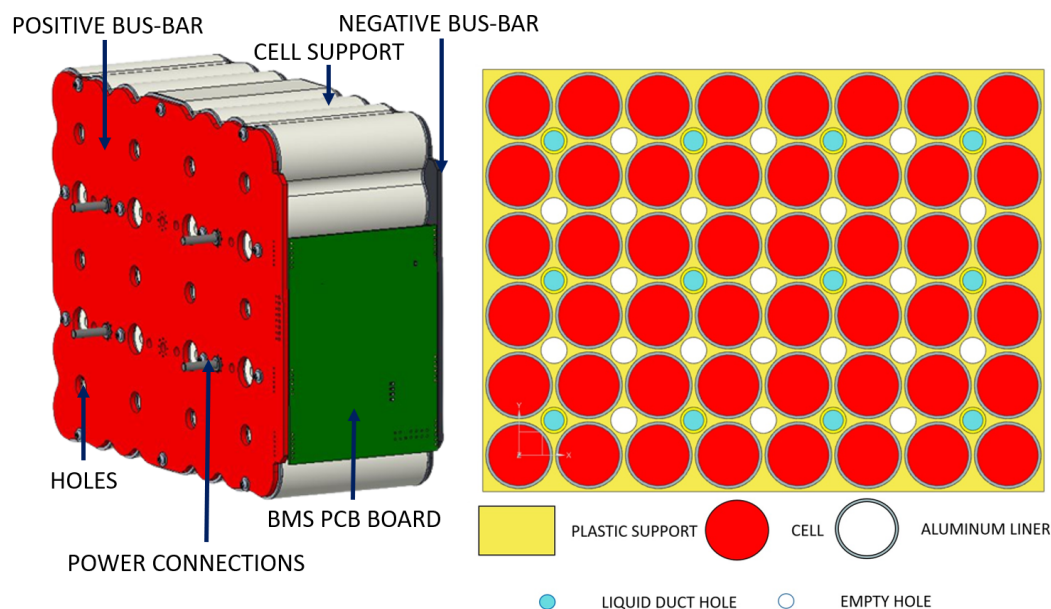

Figure 2. A scheme of the *LiBER* brick (**left**) and a section of the *LiBER* brick plastic support (**right**).

The analysis is divided into five main research macro-topics usually taken into consideration in this genre of studies [59]: the cells support, the Li-ion cells, the BMS system, the liquid-based BTMS and the container. The other parts of the BP, such as the electrical components (fuses, switches, connectors) are not considered in this LCA analysis. The LCA is conducted as a cradle-to-gate analysis (a partial cradle-to-grave without the study of the product disposal) and, concerning the kind of resultant impact, the *ED* and the *GWP* values are considered.

2.1. Cells Support

In Figure 2, a section of the *LiBER* cells support is shown: it is a plastic structure with 48 holes for the Li-ion cells arranged in a 6×8 configuration and one aluminum liner in each hole to better dissipate the heat generated by the cells. About the aluminum, it is assumed to be all primary aluminum as the majority of the literature data about the impact evaluations (ED and GWP) deal with that kind of metal. The LCA about the plastic part of the support involves the analysis of two different materials: the polyoxymethylene (POM) usually used in the manual production line and the ABS common in the automatic production line.

2.2. Li-Ion Cells

The cells chosen for this LCA analysis are the cylindrical *INR* 21700 *P42A* produced by *Molicel* [60] and based on $LiNiMnCoO_2$ cathode. This kind of cells is a quite common choice in the BP mass production when frequent charging/discharging cycles are required (energy storage, automotive): the reason is that the low cobalt content brings to lower costs [61]. The *LiBER* BP concept and assembly processes do not depend on the cells used. Then, the study presented in this paper is designed so that the section concerning the cradle-to-gate analysis of the Li-ion cells can be replaced with a new one focused on a different type of cells instead of the ones analyzed in this work, with the other sections remaining the same. It has to be specified that the following analysis does not take into account

the environmental impacts coming from the use of the Li-ion cells (charging/discharging phases), as well as the battery post-processing. In addition to the anode and the cathode components, the study of a cell deals with many other materials: the constituents of the binder, the separator ones, the electrolyte salt and its additives, and, enclosing the whole assembly, the nickel-plated steel cell casing. Before starting with the impact evaluation some assumptions are completed: the binder is considered as made of polyvinylidene fluoride (PVDF) and represents a negligible mass percentage ($<1\%$) [60] in the selected NMC cells [59]; among the data found in the literature, a separator composition equal to 50% of polypropylene (PP) and 50% of polyethylene (PE) is selected; the electrolyte solvent is considered as 50% dimethyl carbonate (DMC) made and 50% ethylene carbonate (EC) made as the other carbonates which usually compose the NMC cell solvent are in much lower and negligible percentages. Furthermore, the cell casing is not taken into account as in the overall CO_2 emissions balance its impact is lower than 1% [59]. The resulting inventory includes: the anode (graphite coating on a copper foil), the cathode (cobalt(III) lithium oxide ($CoLiO_2$), Mn, Ni coating on an Al foil), the electrolyte salt $LiPF_6$ (lithium hexafluorophosphate), and the electrolyte solvent (50% DMC, 50% EC) [60]. Studies demonstrate that the ED and CO_2 emissions related to the cell assembly are much lower than the those coming from the cell processing (in particular, the processes involving the anode and the cathode) [45]. Other studies highlight how reasonable this thesis is compared to the extremely low emissions for the entire BP assembly and those associated with the overall LCA ($GWP_{ASSEM} \simeq 0.7 \cdot GWP_{TOT}$) [62]. Finally, in this study the manufacturing phase is evaluated only concerning the Li-ion cells, instead this contribution is considered irrelevant regarding the cells support and the liquid-cooled BTMS.

2.3. BMS

Each brick is realized with a 1.8 mm thick FR4 layer and a 35 µm copper thick sheet.

2.4. Liquid-Cooled BTMS

The BTMS considered in this study is based on the real liquid cooling system installed on the *LiBER* BP prototype: it is a water-based BTMS with a coolant circuit made of a silicone rubber tube passing through the holes of the brick. As seen in the brick scheme (Figure 2), among the bigger holes for the cells there are smaller ones for the cooling circuit which passes through 12 of them while the coolant flows along it. The liquid duct holes have a diameter $d_{hole} = 10$ mm, so the chosen silicone rubber tube has an external and an internal diameter equal to $d_{tube, ext} = 10$ mm and $d_{tube, int} = 8$ mm, respectively, resulting in a thickness $s_{tube} = 1$ mm. The LCA regarding the BTMS is here facilitated just considering the silicon rubber tube in terms of raw materials extraction, processing and transportation.

2.5. Container

The battery pack container is made of pultruded composite materials and it has also a structural function. The container cap is not considered as it gives a negligible contribution with modules composed of a high number of bricks.

2.6. LCA Approach

The system boundary of the study comes from a cradle-to-gate approach: it starts with the extraction of the raw materials and ends with the assembly of the BP module. Figure 3 depicts the system boundary and shows the details of the sections present in this work.
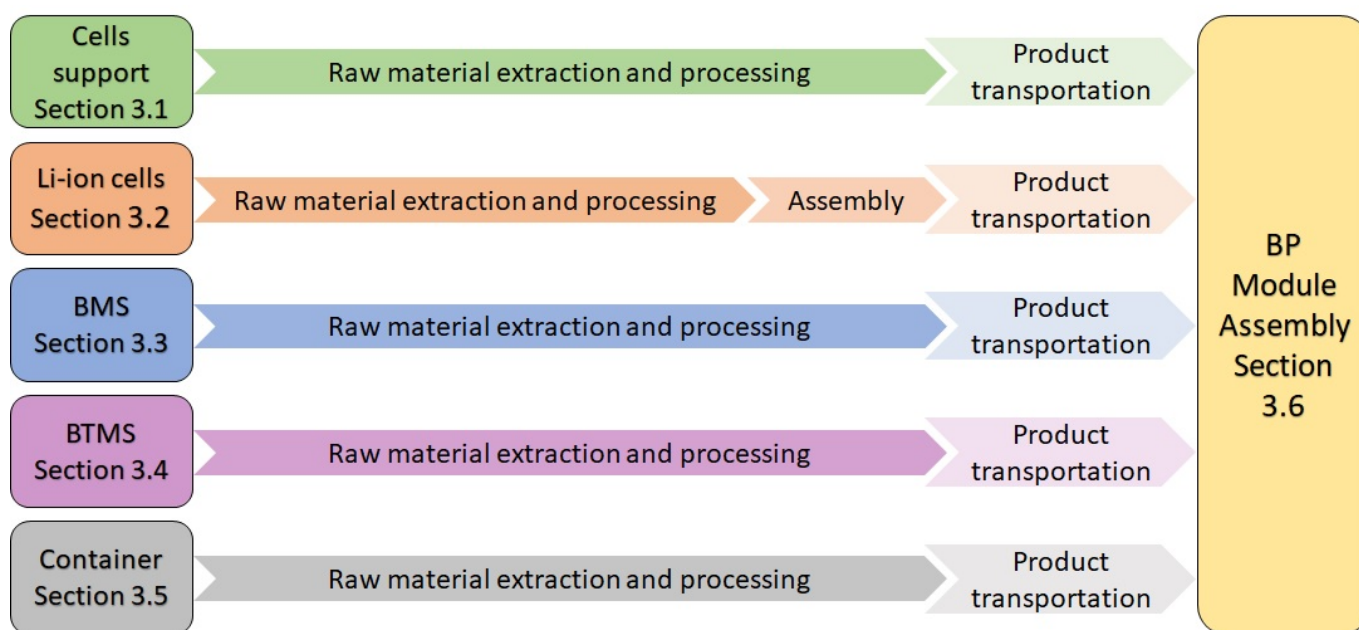
Figure 3. A scheme of the LCA analysis carried on in the paper.

3. Results

3.1. Cell Support

3.1.1. Cell Support: Raw Material Extraction and Processing

Aluminum The production processes involving the primary aluminum are the bauxite extraction, the Bayer (the conversion from bauxite to alumina), and the Hall–Héroult process (the smelting of the alumina into molten cryolite, followed by the electrolysis of the molten salt bath) [63]. Then comes the T6 temper, a heat treatment which consists of two phases: the quenching (a heating process followed by a sudden cooling) and the artificial ageing [64]. The *ED* related to the aluminum cutting process is considered negligible.

POM A block of 4 kg of material is obtained starting from the coarse powder, thanks to a molding process [65]. Then, the block is machined with a CNC miller, removing the chips. During the machining process there is an 80% volume reduction: in order to obtain a realistic analysis, the overall machining process is split into a coarse machining for the 85% of the removed volume, and a fine machining for the 15% of it, resulting in a matrix of 0.8 kg.

ABS The UL 94 V0 is chosen according to the Standard for Safety of Flammability of Plastic Materials: this kind of ABS shows great performances in case of fire emergency, succeeding in stopping the burning process on a vertical specimen within 10 s [66]. The ABS processes deal with a coarse powder molding phase carried on with a hot chamber injection molding method [65]: this means that the ABS gross mass before the process is equal to the ABS net mass after the injection.

The *ED* and the *GWP* values related to the aluminum, POM, and ABS raw materials extraction and processes are summarized in Table 1 and shown in Figure 4 and Figure 5 per unit of mass and energy, respectively.

Table 1. Average *ED* and *GWP* related to the aluminum, POM, and ABS processes [67–71].

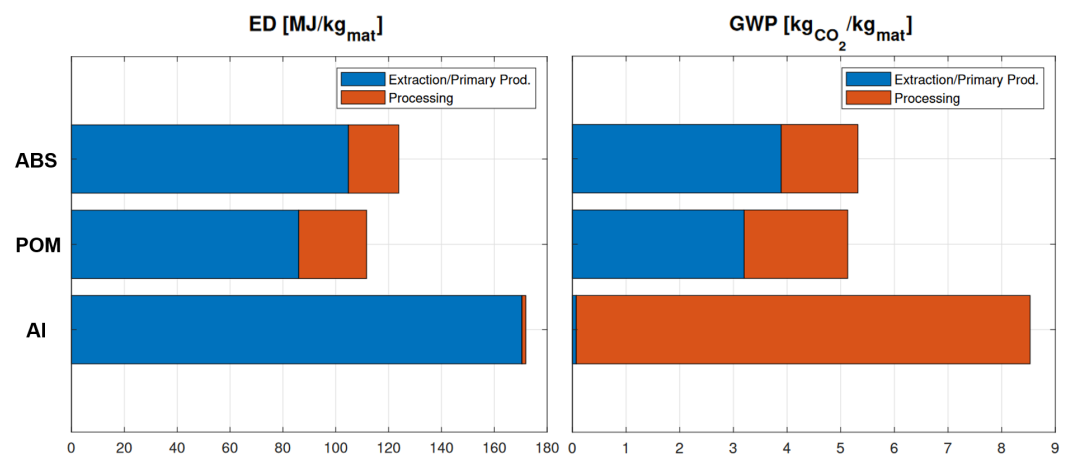|		ED [MJ/Brick]	GWP [kg$_{CO_2}$/Brick]
Al	Extraction	0.52	0.03
	Processing and heat treatments	84.54	4.22
	Coarse machining	0.73	—
	Total	85.79	4.25
POM	Primary production	344.00	12.80
	Block molding	64.00	4.80
	Coarse machining	3.50	0.27
	Fine machining	4.02	0.30
	Total	415.52	18.17
ABS	Primary production	83.84	3.11
	Injection molding	15.24	1.14
	Total	99.08	4.25

Figure 4. Average *ED* and *GWP* per unit of mass related to the ABS, POM, and aluminum extraction and primary production processes.
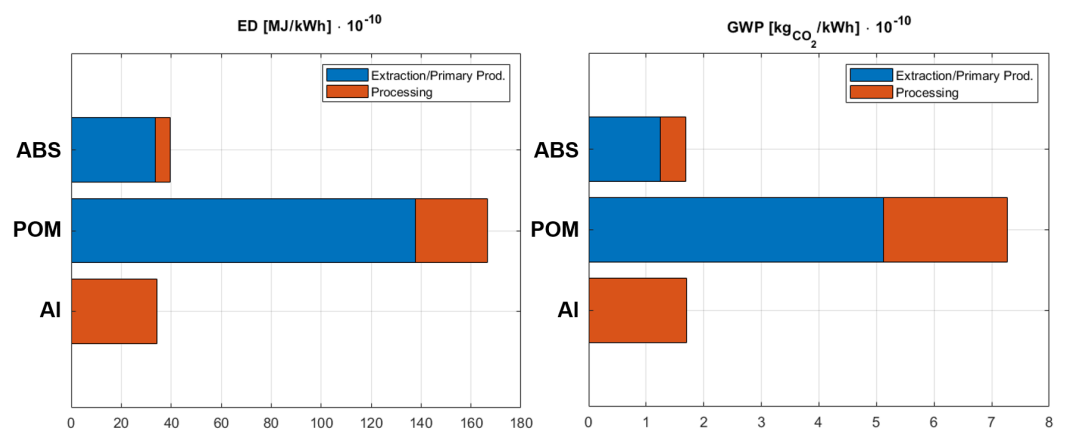

Figure 5. Average *ED* and *GWP* per unit of energy related to the ABS, POM, and aluminum extraction and primary production processes.

3.1.2. Cells Support: Material Transportation

The transportation impact is evaluated considering a diesel powered *IVECO ECOS-TRALIS Active AS* truck for the road transport (whose maximum payload is 10,200 kg) and a HFO powered *MAN S90ME-C9.2-GI* ship for the sea transport, a 8000 *TEU* (Twenty-foot Equivalent Unit) cargo provided with a two-stroke marine engine [72]. The 1 *TEU* represents the dimension of an ordinary container whose maximum payload is 24,000 kg. As the *LiBER* headquarter is based in Bologna (Emilia-Romagna, Italy), this has influenced the choice of where stocking up the materials, aiming to obtain as low transport emissions as possible. The data related to the impact of the transportation means are shown in Tables 2 and 3.

Regarding the aluminum transportation impact, two options are considered. The first one involves the transport of the Al6065: this kind of metal is that selected for the real *LiBER* brick but it is expected that it gives a remarkably negative contribution to the emissions due to the distance of the current stocking up site (Jiangsu, China). The second option is the Al6063: with almost the same mechanical and physical characteristics of the Al6065, this metal can be a possible substitute as it is available in Italy (San Colombano al Lambro). Regarding the plastic materials, both the ABS and the POM are available in Italy at a relatively short distance from Bologna. The calculations for the transport emissions are shown step by step into the Supplementary Material, to be taken as example for all the other transport contributions.

Table 2. Impact evaluation data of a diesel powered *IVECO ECOSTRALIS Active AS* truck considering a payload of 10,200 kg.

	Unit	Value
Emissions	$[\text{kg}_{CO_2}/\text{L}]$	2.65
Fuel consumption	$[\text{L}/\text{km}]$	0.3
Fuel calorific value	$[\text{MJ}/\text{kg}]$	45
Fuel density	$[\text{kg}/\text{L}]$	0.83

Table 3. Impact evaluation data of a HFO powered *MAN S90ME-C9.2-GI* cargo ship considering an average speed $\tilde{v}_{\text{cargo}}$ = 23.5 kn = 43.6 km/h [73].

	Unit	Value
Emissions	$[\text{g}_{CO_2}/\text{km t}]$	12.5
Fuel consumption	$[\text{t}/\text{d}]$	206.8
Fuel calorific value	$[\text{MJ}/\text{kg}]$	42.7

Aluminum 6065 Choosing the Al6065 it is necessary to use both the cargo ship and the truck to import the material from China (total distance s_{cargo} = 19,535 km). The calculations for the transport evaluation impact are reported in the Supplementary Material. The overall *ED* and *GWP* specific values for the Al6065 are the sum of the cargo and the truck contributions: $GWP_{\text{s, Al6065}}$ = 0.366 $\text{kg}_{CO_2}/\text{kg}_{Al}$, $ED_{\text{s, Al6065}}$ = 2.579 MJ/kg_{Al}.

Aluminum 6063 With the same logic, the *ED* and *GWP* values are calculated for the Al6063, considering a travel distance s_{truck} = 175 km. In this case $GWP_{\text{s, Al6063}}$ = 0.013 $\text{kg}_{CO_2}/\text{kg}_{Al}$, $ED_{\text{s, Al6063}}$ = 0.196 MJ/kg_{Al}.

POM Studying the most common trade routes, it is assumed that the POM comes from Brescia (Italy) and travels along the Brescia–Minerbio–Bologna route (s_{POM} = 238 km). Considering this, the specific and the overall *ED* and *GWP* values are calculated obtaining: $GWP_{\text{TOT, POM}}$ = 189 kg_{CO_2}, $GWP_{\text{s, POM}}$ = 0.018 $\text{kg}_{CO_2}/\text{kg}_{POM}$, CED_{POM} = 2723.4 MJ, $ED_{\text{s, POM}}$ = 0.267 MJ/kg_{POM}.

ABS Brescia is chosen as stocking up site for the ABS too but, this time, following the route Brescia–Ravenna–Bologna (s_{ABS} = 353 km). For the ABS it is found: $GWP_{\text{TOT, ABS}}$ =

280.63 kg$_{CO_2}$, $GWP_{s, ABS} = 0.028$ kg$_{CO_2}$/kg$_{ABS}$, $CED_{ABS} = 3978$ MJ, $ED_{s, ABS} = 0.390$ MJ/kg$_{ABS}$.

All the results regarding the transportation impact related to the materials needed for the cells support (negligible if compared with the values in Table 1) are collected in Table 4.

Table 4. Average *ED* and *GWP* related to the transportation impact of the cells support materials.

		ED [MJ/kg$_{material}$]		GWP [kg$_{CO_2}$/kg$_{material}$]	
		TRUCK	**CARGO**	**TRUCK**	**CARGO**
Materials	Al6065	1.72	0.86	0.12	0.24
	Al6063	0.20	–	0.01	–
	POM	0.27	–	0.02	–
	ABS	0.40	–	0.03	–

3.2. Li-Ion Cells

3.2.1. Li-Ion Cells: Raw Material Extraction

Aluminum For the aluminum extraction it is found that $GWP_{s, Al} = 0.078$ kg$_{CO_2}$/kg$_{Al}$; $ED_{s, Al} = 1.040$ MJ/kg$_{Al}$ [68].

Copper The copper extraction process first involves sulphide ores which, then, are processed to become pure copper (Section 3.2.2). For the copper (sulphide ores) extraction, it is estimated that $GWP_{s, Cu} = 1.20$ kg$_{CO_2}$/kg$_{Cu}$; $ED_{s, Cu} = 28.3$ MJ/kg$_{Cu}$ [74].

Lithium Lithium is usually obtained via brine evaporation or it is extracted mining a pegmatite rock (spodumene or petalite) [75]. A brine extraction is possible in presence of saline lakes, seawater, saline sedimentary basins, and wherever high-$NaCl$-concentration solutions are available. This extraction method is based on the natural ores leaching from the Andes mountain range, accumulated underground as brines [76] and then pumped to the surface [77]. The brine is stored inside open pools under the sun, so that the salt concentration increases thanks to the evaporation. The Chilean brines located in the Atacama desert are natural water solutions characterized by the highest content of *Li* and *P* and represent the largest lithium extraction site in the world [76] (from 70% up to 80% of lithium is recovered from brines located in the so-called South America's lithium triangle of Chile, Argentina and Bolivia [78,79]).

In Figure 6, this geographical area is shown and the most important extraction sites are put in evidence. The exploitation of spodumene or petalite ores happens in open-pit mines and it is more common in countries, such as Bolivia, Zimbawe, Australia, Canada, and Portugal. Both of these extraction methods lead to obtain lithium carbonate (Li_2CO_3) and are not so different in terms of environmental impact [75,80] considering favorable weather conditions. On the contrary, Stamp et al. [80] demonstrates that unfavorable conditions, such as the solar discontinuity and the consequent inefficient evaporation, make the ore extraction choice the best one. In this LCA study, a brine extraction carried on with favorable conditions is considered and it is found $GWP_{s, Li} = 4.50$ kg$_{CO_2}$/kg$_{Li}$ [77,81]; $ED_{s, Li} = 31.15$ MJ/kg$_{Li}$ [80]. The choice of the Atacama desert as lithium extraction site represents an important contribution in terms of transportation impact (Section 3.2.4). To minimize the emissions coming from the transport of the other raw materials for the cells it is considered that these elements are all available in Chile. This is a reasonable hypothesis considering how rich is the Chilean land in terms of ores and metals [82–85].
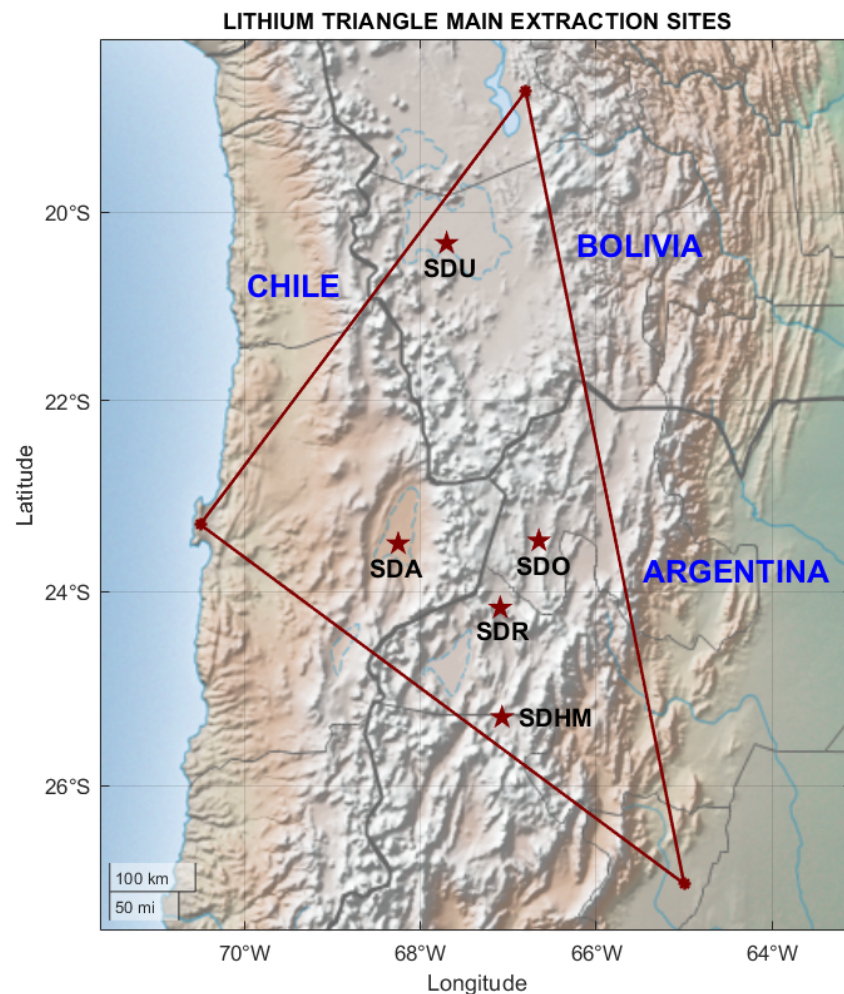
LITHIUM TRIANGLE MAIN EXTRACTION SITES

Figure 6. The South America's lithium triangle holds the most important lithium extraction sites: Salar de Atacama (SDA), Salar del Hombre Muerto (SDHM), Salar de Uyuni (SDU), Salar de Olaroz (SDO), and Salar del Rincon (SDR).

Cobalt This element is produced worldwide as a byproduct of copper, nickel and silver, and copper-cobalt ores are the most common source where it is possible to extract this material [86]. Cobalt is never used alone but it is needed to produce NMC powder, starting from cobalt(II) sulfate ($CoSO_4$) which is then mixed with nickel(II) sulfate ($NiSO_4$), manganese(II) sulfate ($MnSO_4$) and other chemical compounds present in lower quantities. For the cobalt extraction it is found $GWP_{s,\,Co} = 38\,\text{kg}_{CO_2}/\text{kg}_{Co}$; $ED_{s,\,Co} = 653\,\text{MJ}/\text{kg}_{Co}$ [87].

Manganese This is a very abundant element on Earth, available in more than 30 countries. The manganese is extracted from open-pit mines where there is usually a mixture of several manganese oxides, such as pyrolusite, romanechite, manganite: considering the battery cells, the manganese is used as MnO_2, that is the pyrolusite composition. After the extraction, several steps follow (beneficiation, smelting, refining [75]) before obtaining the manganese. The final results for the extraction are: $GWP_{s,\,Mn} = 6.20\,\text{kg}_{CO_2}/\text{kg}_{Mn}$ [75]; $ED_{s,\,Mn} = 16.5\,\text{MJ}/\text{kg}_{Mn}$ [88].

Nickel Nickel is the most important material in terms of cathode mass: as a matter of fact, a NMC cathode is 80% nickel made [89]. Further, it is a natural source and so fully recyclable, not showing quality and performance decrease issues. For the nickel extraction there is $GWP_{s,\,Ni} = 8.84\,\text{kg}_{CO_2}/\text{kg}_{Ni}$; $ED_{s,\,Ni} = 155\,\text{MJ}/\text{kg}_{Ni}$ [90].

Graphite This is the most stable form of coal (in standard conditions) and it is possible to extract it from open-pit mines or from the underground. There are two kind of graphite, the natural and the synthetic one: both produce almost the same CO_2 emissions [91].

Considering the *Molicel* datasheet [60], synthetic graphite is chosen as anode constituent for this study. For the synthetic graphite extraction it is found $GWP_{s,C} = 1.80 \div 8.20$ kg_{CO_2}/kg_C [75]; $ED_{s,C} = 4.80 \div 5.20 \, MJ/kg_C$ [86].

All the results regarding the extraction impact related to the materials needed for the cells are collected in Table 5 which shows the values of both *ED* and *GWP*.

3.2.2. Li-Ion Cells: Material Processing

Lithium carbonate Once the brine is stored in the open pools (Section 3.2.1) the purification occurs (it takes about one year): this is the phase when the lithium concentration increases [77]. Then, a carbonation process follows [80]: this chemical reaction involves lithium (*Li*) and sodium carbonate (Na_2CO_3), producing lithium carbonate (Li_2CO_3) whose production chain proceeds with the compound filtration and washing and, finally, it ends with the packaging phase. For the Li_2CO_3 processing it is: $GWP_{s,Li_2CO_3} = 2.02$ $kg_{CO_2}/kg_{Li_2CO_3}$; $ED_{s,Li_2CO_3} = 28.43 \, MJ/kg_{Li_2CO_3}$ [80]. Li_2CO_3 is then used in the chemical processes to obtain the cathode powders.

Anode graphite powder The synthetic graphite preparation deals with several phases, such as the initial petroleum coke grinding and sizing, and the following mixing where the coke is blended with pitch in the desired proportion. After an extrusion process, the mixture is heated at $800 \div 1000$ °C in a natural-gas-fired furnace. This baking phase is often doubled, putting in the middle a further impregnation phase: the mixture is blended with more pitch to improve the final graphite properties. Finally, the graphitization occurs: this fully electricity powered phase slowly brings the product to 3000 °C, so the graphite crystal formation can start [86]. For the anode graphite processing it is: $GWP_{s,gr} = 4.86$ kg_{CO_2}/kg_{gr}; $ED_{s,gr} = 89.87 \, MJ/kg_{gr}$ [91].

Copper anode current collector After the extraction of the sulphide ores, several processing stages occur: the beneficiation to transform the ores into a slurry [75], the drying and the smelting. Then, for the copper anode collector a refining phase is fundamental. All the aforementioned stages and the related impacts are discussed more in detail in the Supplementary Material. For the copper current collector processing it is found: $GWP_{s,Cu_{anod}} = 4.1 \, kg_{CO_2}/kg_{Cu_{anod}}$; $ED_{s,Cu_{anod}} = 47 \, MJ/kg_{Cu_{anod}}$ [92].

Cathode Ni–Mn–Co powders The most common cathode composition in NMC batteries is that of the NMC111 cells (also called NMC333) which means that the *Ni–Mn–Co* blend is in the ratio 1:1:1 [93,94]. Regarding the impact evaluation of the cathode powder, discordant results are present in the literature if considering analytical [95] or experimental investigations [91]: experimental results are taken into account in this paper and the detailed reactions to obtain these powders are discussed in the Supplementary Material. For the *Ni–Mn–Co* cathode powders processing it is $GWP_{s,Ni–Mn–Co} = 16.11 \, kg_{CO_2}/kg_{Ni–Mn–Co}$; $ED_{s,Ni–Mn–Co} = 231.28 \, MJ/kg_{Ni–Mn–Co}$ [91].

Aluminum cathode current collector The raw aluminum is processed (see Section 3.1.1) till reaching the ingot casting [75]. Then, the ingot has to be processed too as the thickness of the final product has to decrease until about $10 \div 20$ μm [96]. To do this, multiple rolling stages are necessary. The aluminum rolling exploits steel rolls to dramatically reduce the ingot thickness which usually ranges from 0.46 m to 0.76 m [68]. All the aluminum rolling operations are deepened into the Supplementary Material. Considering all the processes after the mining until the rolling (included), results are: $GWP_{s,Al_{cath}} = 8.86 \, kg_{CO_2}/kg_{Al_{cath}}$; $ED_{s,Al_{cath}} = 137.06 \, MJ/kg_{Al_{cath}}$ [68].

PP and PE separators As the separator is 50% PP and 50% PE made, both kinds of plastic processes are considered so that $GWP_{s,PP} = 2.53 \, kg_{CO_2}/kg_{PP}$; $ED_{s,PP} = 78.59$ MJ/kg_{PP}; $GWP_{s,PE} = 2.93 \, kg_{CO_2}/kg_{PE}$; $ED_{s,PE} = 80.96 \, MJ/kg_{PE}$ [91].

Electrolyte salt The electrolyte salt is made of lithium hexafluorophosphate ($LiPF_6$): it is the reaction product between the phosphorous pentafluoride (PF_5) and the lithium fluoride (*LiF*) previously dissolved in hydrogen fluoride (*HF*) [97]. For the electrolyte salt processing it is: $GWP_{s,LiPF_6} = 12.15 \, kg_{CO_2}/kg_{LiPF_6}$; $ED_{s,LiPF_6} = 179.07 \, MJ/kg_{LiPF_6}$ [91].

DMC and EC electrolyte solvents Mixing DMC and EC with $LiPF_6$ allows increasing the permittivity of the electrolyte salt [98]. For the electrolyte solvent processing it is found: $GWP_{s, DMC} = 1.72$ kg$_{CO_2}$/kg$_{DMC}$; $ED_{s, DMC} = 37.44$ MJ/kg$_{DMC}$; $GWP_{s, EC} = 0.47$ kg$_{CO_2}$/kg$_{EC}$; $ED_{s, EC} = 10.19$ MJ/kg$_{EC}$ [91].

All the results regarding the processing impact related to the material transformations needed for the cells are collected in Table 5.

Table 5. Average *ED* and *GWP* related to the extraction and processing of the raw materials for one cell.

	Materials	ED [MJ/Cell]	GWP [kg$_{CO_2}$/Cell]
Extraction	Al	0.015	0.080
	Cu	0.267	0.011
	Li	0.065	0.009
	Co	4.571	0.266
	Mn	0.116	0.043
	Ni	1.085	0.062
	Graphite	0.053	0.053
	Total	6.171	0.446
Processing	Li$_2$CO$_3$	0.060	0.004
	Anode graphite powder	0.944	0.051
	Cu anode collector	0.444	0.0387
	Cathode Ni–Mn–Co powder	4.857	0.338
	Al cathode collector	1.919	0.124
	PP separator	0.149	0.0048
	PE separator	0.153	0.0055
	Electrolyte salt	0.376	0.025
	DMC electrolyte solvent	0.157	0.007
	EC electrolyte solvent	0.043	0.002
	Total	9.459	0.626

3.2.3. Li-Ion Cells: Product Assembly

The manufacturing of the cells is carried out in a large scale and fully automated production site. The process consists of several operations, such as the manufacturing of the electrodes, and the assembly and the finishing of the cells [99]. Independently from the shape of the cells (cylindrical, pouch, prismatic) the electrodes manufacturing always includes the following steps: the mixing of the powders with additives using intensive mixers and dispersers; the coating of the *Al* and *Cu* electrode foils (the collectors) with the powder mixture already obtained (Section 3.2.2); the drying of the resulting collectors, a thermal cycle (50 ÷ 180 °C) useful to improve the quality of the coating and the finishing of the surface; the calendering (compression and cleaning) and the slitting (cutting, cleaning and winding) stages. In a NMC111 cell with a graphite anode, the higher active mass of the cathode with respect to the anode one results in lower *ED* values for the anode manufacturing stages. The subsequent steps are specific for cylindrical cells and deal with the assembly of the cells: the winding of the electrodes with the separator (realization of the jelly roll); the packing during which the jelly roll is inserted into the nickel plated steel casing, welded to its top and bottom and sealed in it; the vacuum and the under-pressure filling processes to inject a precise amount of electrolyte into the cell by means of vibrating tables; the final cell sealing. Regarding the finishing operations for cylindrical cells there are the SEI (solid electrolyte interphase) formation; the ageing process at high (30 ÷ 50 °C) or environmental temperatures which lasts 1.5–3 weeks; the quality control (tests about the cell characterization); and other possible complementary steps to manage the air conditions inside the clean rooms used for the assembly process. Considering literature results [45,99] normalized for 1 Wh cells and scaling them for this case study about *INR* 21700 *P42A* cells (15.12 Wh/cell), it is possible to estimate the *ED* values in terms of Wh and then

converting them into *MJ* to know how much energy per cell (MJ/cell) is used. Among all the *ED* contributions it has to be highlighted that the drying one is the less precise as strongly influenced by the environmental conditions and the machines used. As a matter of fact, literature data related to this process greatly differ from each other. The estimation of the *GWP* values is much more difficult due to the lack of papers which deepen the assembly CO_2 emissions. The reason is that it is hard to obtain reasonable *GWP* average values which take into account all the different existent technologies used for these stages. Further, the complexity in evaluating the power needed by all the machines (mixers, centrifuges, ovens) and the fact that they rarely work at standard conditions and/or continuously (sometimes they are in standby) make the evaluations even harder. Results in Table 6 are referred to by a single cell, the weight of which is $w_{cell} = 70$ g [100], so the approximated *ED* and *GWP* values related to 1 kg of cells are $ED_{assem} = 28.84$ MJ/kg_{cell} $GWP_{assem} = 0.9929$ kg_{CO_2}/kg_{cell}. For the same reason as is explained in Section 3.2.1, to lower the transportation impact the whole cell assembly process is intended as completely carried out in Chile. In this way, it is possible not to consider transportation impacts related to the routes from the assembly sites (different from Chile) to the purchaser location (Bologna). The assumption of a single geographical site as an extraction, processing, and assembling place is reasonable considering the increasing amount of companies and institutions which commission investigations about the economical benefits coming from this strategy [79]. Results related to the impact of the electrode manufacturing (EM), the cells assembly (CA), and cells finishing (CF) are shown in Table 6.

Table 6. Average *ED* and *GWP* related to the assembly stages of the cells.

		Assembly Stages	ED [MJ/Cell]	GWP [kg_{CO_2}/Cell]
EM	Anode	Mixing	0.0020	*n.a.*
		Coating	0.0004	*n.a.*
		Drying	0.2856	*n.a.*
		Calendering	0.0001	*n.a.*
		Slitting	*negl.*	*n.a.*
	Cathode	Mixing	0.0036	*n.a.*
		Coating	0.0004	*n.a.*
		Drying	0.8893	*n.a.*
		Calendering	0.0001	*n.a.*
		Slitting	*negl.*	*n.a.*
CA		Winding	0.0136	0.0011
		Filling and packing	0.0865	0.0073
		Washing	0.1078	0.0091
CF		SEI formation	0.5536	0.0462
		Aging	0.0218	0.0012
		Testing	0.0539	0.0046
		Total	2.0187	0.0695

3.2.4. Li-Ion Cells: Product Transportation

In this evaluation, the same logic used for the cells support transportation impact (Section 3.1.2) is followed. Among the most common existing trade routes, the chosen one is Santiago de Compostela (Chile) to Rio Grande do Sul (Brasil) to Antwerp (Belgium) to Bologna (Italy), with the first and the third road stages and one sea stage in the middle. The *ED* and *GWP* values related to the transportation impact of the cells are collected in Table 7 considering all the travelled stages by truck or cargo: the first road stage T1, the second sea stage C and the third road stage T2 (see Supplementary Material for the all the partial *ED* and *GWP* contributions).

The overall results related to the cells raw materials extraction and processing, to the product assembly and transportation are shown in Figure 7.

Table 7. Average *ED* and *GWP* related to the transportation of the cells considering all the travelled stages.

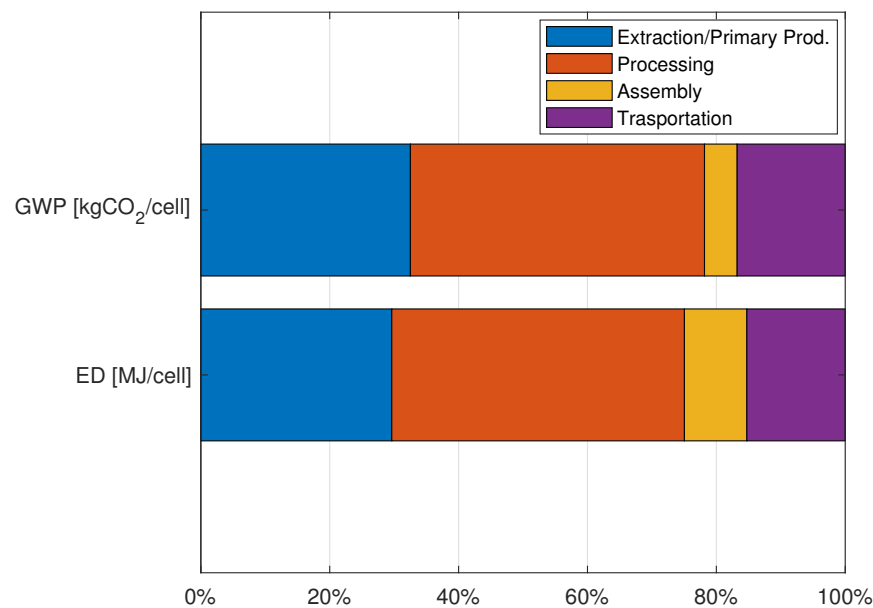| Route	ED [MJ/Cell]	GWP [kg$_{CO_2}$/Cell]
T1	2.080	0.148
C	0.022	0.006
T2	1.076	0.076
Total	3.179	0.230

Figure 7. Average *ED* and *GWP* related to the raw materials extraction and processing, and the assembly and transportation of the cells.

3.3. BMS

3.3.1. BMS: Raw Material Extraction and Processing

The circuits and components of the electronic boards are made of copper, aluminum, silicon, and ceramic (X7R) and the boards are realized with glass-reinforced laminate material (FR4). For the evaluations of the copper and the aluminum extraction and processing, the discussion presented in Sections 3.2.1 and 3.2.2 is taken as reference. The X7R is a multi-layer material used for the capacitors electrodes. It is composed of barium carbonate ($BaCO_3$), titanium (IV) oxide (TiO_2), dysprosium(III) oxide (Dy_2O_3), and borosilicate glass. There is also the usage of a solvent (methyl ethyl ketone), a cationic polymeric dispersant (Hypermer KD1), a plasticizer (PEG-400), and a binder (Butvar). The total carbon footprint is $GWP_{s, BMS, X7R} = 4.19$ kg$_{CO_2}$/kg$_{X7R}$ [101]. The process for the X7R production involves a drying and a sintering stage, with a correspondent energy demand value of $ED_{s, BMS_1, X7R} = 79.56$ MJ/kg$_{X7R}$. To produce X7R capacitors some auxiliary processes are needed, such as milling and tape-casting: their contribution is equal to $ED_{s, BMS_2, X7R} = 12.24$ MJ/kg$_{X7R}$. All the results regarding the raw material extraction and processing impacts related to the BMS are collected in Table 8.

Table 8. Average *ED* and *GWP* related to the extraction and processing of the raw materials for the BMS of one brick.

	Materials	ED [MJ/Brick]	GWP [kg$_{CO_2}$/Brick]
Extraction	Al	0.034	0.001
	Cu	3.633	0.154
	Ni	2.089	0.118
	Si	0.444	0.053
	X7R	0.792	0.009
	FR4	0.108	0.060
	Total	7.100	0.395
Processing	Al	0.682	0.112
	Cu	0.109	0.539
	Ni	1.044	0.119
	Si	0.444	0.066
	X7R	0.122	0.177
	FR4	0.108	0.001
	Total	2.510	1.015

3.3.2. BMS: Product Transportation

The city of Regensburg (Germany) is chosen as a FR4 production site as it represents the headquarter of one of the biggest factories in Europe. The distance from Regensburg to Bologna is equal to 692 km and for this route it is found: $ED_{s, BMS} = 0.76$ MJ/kg$_{BMS}$ and $GWP_{s, BMS} = 0.054$ kg$_{CO_2}$/kg$_{BMS}$. As links and BMS boards contain 129 g and 20 g of FR4, respectively, (the $1.31 \times 10^{-3}\%$ and the $2 \times 10^{-4}\%$ of the truck payload) and considering th transportation of some other additional components ($1.5 \times 10^{-3}\%$ of the payload), the emissions related to the transportation of each brick are summarized in Table 9.

Table 9. Average *ED* and *GWP* related to the extraction, processing and transportation for the BMS of one brick.

Impact	ED [MJ/Brick]	GWP [kg$_{CO_2}$/Brick]
Extraction and processing	9.610	1.410
Transportation	0.485	0.044
Total	10.095	1.454

3.4. BTMS

3.4.1. BTMS: Raw Material Extraction and Processing

The state of the art about the silicone rubber production impact does not provide any information about the *ED* and *GWP* values which regard the transformation of the raw materials alone: the majority of the papers propose data related to the extraction of the raw materials and their processing together. There are lots of stages before arriving at the silicone rubber tube production: the whole process starts with a thermal phase which involves the silicon(IV) oxide (SiO_2) and allows to obtain silicon metal; then, several other chemical and mechanical processes occur with a descending energy requirement [102]. One of the final products is the silicone rubber, the material used to produce the silicone rubber tubes by extrusion. In the Supplementary Material the attention is focused on the SiO_2 reaction as it is the most energy-intensive process due to the exploitation of a submerged arc furnace (SAF). The overall *ED* and *GWP* values reported in Table 10 regard the entire silicone rubber tube production. Thanks to *openLCA* (an open source software useful to conduct LCA studies) [103] and exploiting the ELCD and the Idemat databases, for the final silicone rubber tube it is found: $GWP_{s, tube} = 3.745$ kg$_{CO_2}$/kg$_{tube}$; $ED_{s, tube} = 118.920$ MJ/kg$_{tube}$ (Table 10).

3.4.2. BTMS: Product Transportation

The selected silicone rubber supplier is located in Milan (Italy) so the transport impact concerns just a road travel (216 km). For the route Milano-Bologna it is found: $GWP_{s,\,tube} = 0.017\ \text{kg}_{CO_2}/\text{kg}_{tube}$; $ED_{s,\,tube} = 0.237\ \text{MJ}/\text{kg}_{tube}$ (Table 10).

Table 10. Average *ED* and *GWP* related to the extraction, processing, and transportation for the silicone rubber tube of the BP liquid cooling system.

Impact	ED [MJ/kg$_{material}$]	GWP [kg$_{CO_2}$/kg$_{material}$]
Extraction + processing	118.92	3.75
Transportation	0.24	0.02
Total	119.16	3.77

High values of *ED* and *GWP* are shown in Table 10 regarding the material extraction and processing to realize the silicone rubber tube of the BTMS. In this case energy-intensive thermal and chemical processes are exploited to obtain the final product, so the aim of reducing the energy demand represents a hard challenge. Further, the use of the SAF does not help in lowering the *GWP*: to face this problem, some effectiveness cutting-edge filters [104] can be used both to reduce CO_2 emissions and to recycle it, transforming this end-of-life (EoL) product in feeding material for the life cycle of a new product.

3.5. Container

3.5.1. Container: Raw Material Extraction and Processing

Composites are made of two or more different materials (fibers and reinforcements), their production techniques are different from the more ordinary ones (metal or polymer processes) and the production rates are not so high. Energy-intensive chemical processes are necessary to realize thermosetting and thermoplastic polymer matrices (the reinforcements) for composite structures, such as the container one. However there are some thermosetting polymers, including polyester and epoxy resins (often used in fiber-reinforced composites), which present relatively low energy intensity values [105]. Once prepared the matrices and after obtaining the fibers there are further stages, such as the textile manufacturing and the pre-preg preparation needed before the fibers are reinforced with the matrix. The impacts related to the raw materials extraction and processing for the BP container results to be: $GWP_{s,\,cont} = 9.104\ \text{kg}_{CO_2}/\text{kg}_{cont}$ and $ED_{s,\,cont} = 169.69\ \text{MJ}/\text{kg}_{cont}$ (Table 11).

3.5.2. Container: Product Transportation

The selected poltruded composite structure supplier is located in Milan (Italy), so the results found in Section 3.4.2 for the BTMS transportation impact are valid for the container transportation impact, too (Table 11).

Table 11. Average *ED* and *GWP* related to the extraction, processing and transportation of the container.

Impact	ED [MJ/kg$_{material}$]	GWP [kg$_{CO_2}$/kg$_{material}$]
Extraction and processing	169.69	9.104
Transportation	0.237	0.017
Total	169.927	9.121

3.6. Module Assembly

The *LiBER* BP module is assembled according to a semi-automatic procedure. In the first automated line, the cells are captured by a Delta robot and placed in the cells support. The electrodes are then laser welded on the PCB. The more energy-intensive stages are

those related to the cells placement and to the electrodes welding but the overall *ED* of these processes is negligible if compared with the contributions assessed in the previous sections. The brick obtained with this automated process is then moved by an operator and inserted into the module container. The whole process is highly innovative and does not require any wires welding. The bricks are easily removable from the final assembly as the entire product is designed with a circular economy approach.

4. Discussion

The results presented in the previous sections can be referred to the whole BP, visualizing the contributions of the five sub-systems, and then discussing the possible strategies to reduce the overall environmental impact. The results related to the entire BP are collected in Table 12 and shown in Figure 8 per unit of energy.

Table 12. *ED* and *GWP* related to the battery pack.

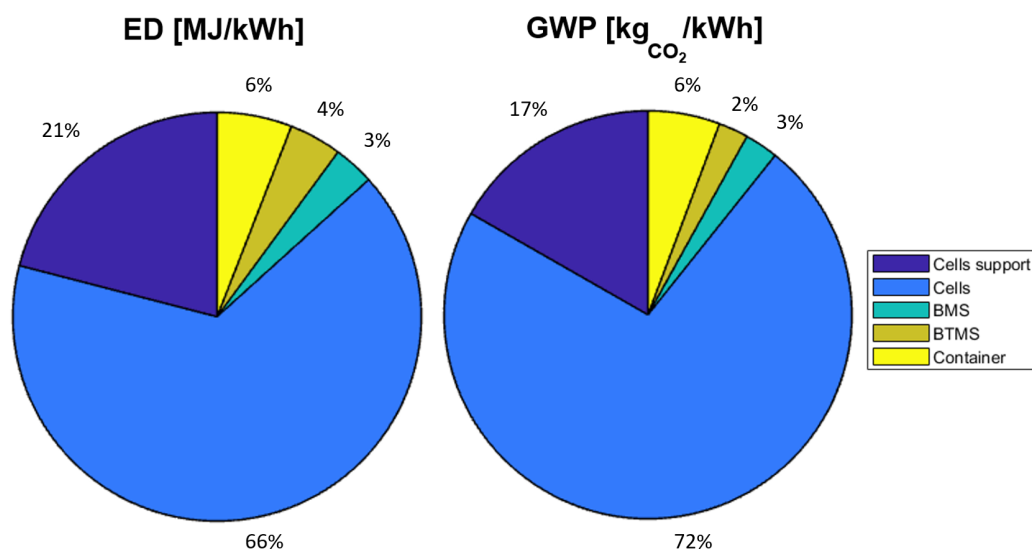| Impact	ED [(MJ/kWh) · 10^{-9}]	GWP [(kg_{CO_2}/kWh) · 10^{-9}]
Cells support	24.084	1.071
Cells	75.474	4.641
BMS	3.677	0.170
BTMS	4.773	0.151
Container	6.806	0.365
Total	114.814	6.398

Figure 8. *ED* and *GWP* per unit of energy related to the entire *LiBER* battery pack.

The contribution of the cells is the most relevant due to the results obtained for the extraction of the raw materials (Table 5). For instance, cobalt extraction has a deep impact in terms of both *ED* and *GWP*, followed by the nickel which has a high *ED* value, too. These are two fundamental elements to produce the cathode powder for the NMC111 cells, so it is not possible to lower this contribution if the use of this kind of cells is mandatory for the application. However, when it is possible to use another type of NMC cells, the more innovative NMC622 or NMC811 batteries represent a better choice. The NMC622 cathode is composed of 60% of *Ni*, 20% of *Mn*, and 20% of *Co*; the NMC811 cathode is composed of 80% of *Ni*, 10% of *Mn*, and 10% of *Co*. Both of them have a lower weight (lower transport impact) and a higher energy density with respect to the NMC111. The extremely reduced quantity of *Co* in NMC811 cells, their lowest weight and highest energy density may suggest that this is the best choice. However, on the other hand, the high *Ni*

percentage is responsible for a more sensitive chemistry and, consequently, the need of additional post-processing phases and a more expensive manufacturing process [94]. Plus, NMC811 cells are sensitive to moisture and air so, in an automotive application, a further sealed structure would be necessary to insulate them from the outside. All these additional processes and components would increase the *ED* and *GWP* values, nullifying the benefits brought by the lower *Co* percentage. From this point of view, the NMC622 represent a good compromise and this is the reason why the *Molicel* cells have been chosen for the *LiBER* BP.

About the processing of the cells materials (Table 5), results show high values of *ED* and *GWP* for several processed materials, but it is possible to lower only some of them. One of the initial assumptions is considering the separator as 50% PP-made and 50% PE-made, but looking at the related *ED* and *GWP*, the results show that the use of a 100% PP-made separator brings to a decrease in both energy demand ($\Delta ED = -2.93\%$) and CO_2 emissions ($\Delta GWP = -13.65\%$). A similar evaluation can be completed regarding the electrolyte solvent which is considered 50% DMC-made and 50% EC-made. The use of a 100% EC-made electrolyte solvent brings to a great decreasing of both energy demand ($\Delta ED = -72.78\%$) and CO_2 emissions ($\Delta GWP = -72.67\%$). The processes regarding the anode and the cathode powders and collectors, as well as the electrolyte salt production are very energy-intensive as they include several thermal, chemical, and electrochemical phases. As these treatments are fundamental for the quality of the final components, the only possible choice to lower the energy demand is the exploitation of the most efficient available industrial plants. Although during the assembly phase there are stages with a higher impact than others, the final *ED* and *GWP* values do not deeply influence the overall results of the LCA study. For this reason, and also because the assembly impact is extremely dependant from several hardly predictable factors, a more effective strategy to lower the whole cycle *ED* and *GWP* is focusing on the other more manageable production steps. Considering the assumption of the cells assembled in Chile, the transportation impact includes both truck and cargo stages. As seen before, the sea transport is a better choice than the road one: although the total distance travelled by the truck (3694 km) represents the 50.68% of the distance travelled by the cargo (7289 km), the sea transport results in great *ED* and *GWP* decreases equal to $\Delta ED = -99.29\%$ and $\Delta GWP = -97.19\%$. So, the more it is possible to exploit the sea transport, the better is in terms of impact. Figure 7 shows that the impact of the cells support is about the 20% of the total ED.

Looking at the results obtained for the extraction and production of the aluminum needed to realize the cells support (Table 1) it is clear that innovative technologies to process the aluminum could represent an efficient solution to lower the *ED* value instead of proceeding with the ordinary and energy-intensive methods (Bayer and Hall–Héroult processes, Section 3). Cutting-edge technologies would be also promising to reduce the CO_2 emissions. Regarding the plastic material for the cells support, the choice is driven by both the *ED* and the *GWP* value. As a matter of fact, comparing *GWP* for POM and ABS in Table 1, results show the values $18.17 \, \mathrm{kg_{CO_2}}$/brick for POM and $4.25 \, \mathrm{kg_{CO_2}}$/brick for ABS, with a percentage decreasing $\Delta GWP = -76.61\%$ choosing ABS. Considering *ED* in Table 1, the obtained values 415.52 MJ/brick for POM and 99.08 MJ/brick result in a percentage decreasing $\Delta ED = -76.16\%$ with ABS. The ABS is definitely the best choice in terms of both *GWP* and *ED*. Analyzing the transportation impact for the materials of the cells support, regarding the aluminum it clearly appears that choosing Al6063 instead of Al6065 represents the more convenient option considering both the energy demand and the emissions. Indeed, the overall Al6063 *ED* results to be $0.2 \, \mathrm{MJ/kg_{Al6063}}$ instead of $2.58 \, \mathrm{MJ/kg_{Al6065}}$ for Al6065, with a percentage decrease $\Delta ED = -92.25\%$ and the overall Al60603 *GWP* results to be $0.01 \, \mathrm{kg_{CO_2}/kg_{Al6063}}$ instead of $0.36 \, \mathrm{kg_{CO_2}/kg_{Al6065}}$ for Al6065, with a percentage decrease $\Delta GWP = -97.22\%$. However, it has to be highlighted how convenient is the cargo transport with respect to the truck one. Focusing on the Al6065 impact values, the results show that the *GWP* for the cargo stage is higher by 50% than that related to the truck stage but the distance travelled by the truck is just the 8.01% of the cargo distance. Further, the *ED* for the cargo stage is lower by 50% than

that related to the truck stage. Hence, if it is possible to choose between a road or a sea transportation, it should be better to go for the second option. Finally, also the module composite container shows a relevant impact (see Figure 7). To lower the environmental impact coming from the composite goods production, EoL recycling stages are fundamental and increasingly adopted as effective strategy [106]. However, there is still a lot to do in the energy saving direction for composite materials. In particular, considering lower energy-intensive composites processes and the production of more sustainable matrices, such as bio-based resins, further investigation needs to be performed to optimize this production field, trying to overcome the existent drawbacks [107].

5. Conclusions

The whole life cycle of a *LiBER* BP unit has been studied, carrying on a LCA evaluation with a cradle-to-gate approach whose result is a series of estimations and suggestions useful to lower both the *ED* and the *GWP* of the entire product chain supply. Five main research macro-topics are considered: the cells support, the Li-ion cells, the BMS, the liquid cooling BTMS and the BP container. After discussing about reasonable assumptions useful for the assessment, the environmental impacts are evaluated focusing on the raw materials extraction and the processing, the assembly of the components and the transportation of the final products. The resulting interpretation proposes alternative methods and choices that can be performed to lower the energy demand and the CO_2 emissions, such as using the ABS instead of the POM as material for the cells support, preferring the sea transport with respect to the road one, choosing low-cobalt cells, using the PP instead of the PE for the separator and the EC instead of the DMC for the electrolyte salt. Finally, good practices would be trying to avoid the extraction and processing of the materials by means of obsolete machines and installing a recycling line in the production plants. The majority of the thermal, chemical, and processes electrochemical are characterized by energy-intensive phases but the choice of cutting-edge technologies could represent a key against the high values of *ED* and *GWP*. The analysis highlights the importance of extending the life span of battery components through the reuse of parts. In this perspective, there are not only possible technological changes but also a mindset switch towards a new cycle of thinking, considering the EoL products as feedstock for the life cycle of the new products.

Abbreviations

The following abbreviations are used in this manuscript:

ABS	Acrylonitrile butadiene styrene
BP	Battery pack
BTMS	Battery thermal management system
CA	Cells assembly
CED	Cumulative energy demand
CF	Cells finishing
CTC	Cradle-to-cradle
CTG	Cradle-to-grave
DMC	Dimethyl carbonate
ED	Energy demand
EC	Ethylene carbonate
EM	Electrode manufacturing
EoL	End of life
EV	Electric vehicle
GWP	Global warming potential
HFO	Heavy fuel oil
ILCD	International Reference Life Cycle Data System
ISO	International Organization for Standardization
LCA	Life cycle assessment
LCI	Life cycle inventory
LCIA	Life cycle impact assessment
LCT	Life cycle thinking
LIB	Lithium-ion battery
LiBER	Lithium Battery for Emilia–Romagna
NMC	Nickel Manganese Cobalt oxide
PCB	Printed circuit board
PE	Polyethylene
POM	Polyoxymethylene
PP	Polypropylene
PVDF	Polyvinylidene fluoride
SAF	Submerged arc furnace
SEI	Solid electrolyte interface
TEU	Twenty-foot Equivalent Unit
UNEP	United Nations Environment Programme

References

1. European Commission. *Communication from the Commission to the European Parliament, the Council, the European Economic and Social Committee and the Committee of the Regions; Towards a Comprehensive Climate Change Agreement in Copenhagen*; Additional Background Information; European Commission: Brussels, Belgium, 2009.
2. *Economia Circolare—Perché "Circolare"*; Circular Economy Network: Rome, Italy, 2018.
3. JCR. *ILCD Handbook: General Guide for Life Cycle Assessment—Provisions and Action Steps*; Publications Office of the European Union: Luxembourg, 2010.
4. Ellen MacArthur Foundation. *Towards a Circular Economy: Business Rationale for an Accelerated Transition*; Ellen MacArthur Foundation: Cowes, UK, 2015.
5. Schulz, M.; Bey, N.; Niero, M.; Hauschild, M. Circular economy considerations in choices of LCA methodology: How to handle EV battery repurposing? *Procedia CIRP* **2020**, *90*, 182–186. [CrossRef]
6. Ashkin, S. *Cradle to Grave vs. Cradle to Cradle*; ClearLink: Salt Lake City, UT, USA, 2008.
7. Li, J.; Xiong, F.; Chen, Z. An integrated life cycle and water footprint assessment of nonfood crops based bioenergy production. *Sci. Rep.* **2021**, *11*, 3912.
8. Gerbens-Leenes, W.; Berger, M.; Allan, J.A. Water footprint and life cycle assessment: The complementary strengths of analyzing global freshwater appropriation and resulting local impacts. *Water* **2021**, *13*, 803. [CrossRef]
9. Trevisan, L.; Bordignon, M. Screening Life Cycle Assessment to compare CO_2 and Greenhouse Gases emissions of air, road, and rail transport: An exploratory study. *Procedia CIRP* **2020**, *90*, 303–309. [CrossRef]
10. Corti, A.; Lombardi, L. End life tyres: Alternative final disposal processes compared by LCA. *Energy* **2004**, *29*, 2089–2108. [CrossRef]

11. Laitala, K.; Klepp, I. Clothing disposal habits and consequences for life cycle assessment (LCA). In *Handbook of Life Cycle Assessment (LCA) of Textiles and Clothing*; Elsevier: Amsterdam, The Netherlands, 2015; pp. 345–365.

12. McDonough, W.; Braungart, M. *Cradle to Cradle: Remaking the Way We Make Things*; North Point Press: New York, NY, USA, 2002.

13. Matthews, H.; Hendrickson, C.; Matthews, D. *Life Cycle Assessment: Quantitative Approaches for Decisions That Matter*; CRC Press: Boca Raton, FL, USA, 2018.

14. Khoo, H.H.; Isoni, V.; Sharratt, P.N. LCI data selection criteria for a multidisciplinary research team: LCA applied to solvents and chemicals. *Sustain. Prod. Consum.* **2018**, *16*, 68–87. [CrossRef]

15. Lupton, R.C.; Allwood, J.M. Hybrid Sankey diagrams: Visual analysis of multidimensional data for understanding resource use. *Resour. Conserv. Recycl.* **2017**, *124*, 141–151. [CrossRef]

16. Baumann, H.; Tillman, A.M. *The Hitch Hiker's Guide to LCA: An Orientation in Life Cycle Assessment Methodology and Application*; Studentlitteratur AB: Lund, Sweden, 2004.

17. Sazdovski, I.; Bala, A.; Fullana-i Palmer, P. Linking LCA literature with circular economy value creation: A review on beverage packaging. *Sci. Total Environ.* **2021**, *771*, 145322. [CrossRef] [PubMed]

18. Scheepens, A.; Vogtländer, J.; Brezet, J. Two life cycle assessment (LCA) based methods to analyse and design complex (regional) circular economy systems. Case: Making water tourism more sustainable. *J. Clean. Prod.* **2016**, *114*, 257–268. [CrossRef]

19. Henry, B.; Russell, S.; Ledgard, S.; Gollnow, S.; Wiedemann, S.; Nebel, B.; Maslen, D.; Swan, P. LCA of wool textiles and clothing. In *Handbook of lIfe Cycle Assessment (LCA) of Textiles and Clothing*; Elsevier: Amsterdam, The Netherlands, 2015; pp. 217–254.

20. Linhares, T.; de Amorim, M.T.P. LCA of textile dyeing with Acacia Dealbata tree bark: a case study research. *Procedia Eng.* **2017**, *200*, 365–369. [CrossRef]

21. Lamnatou, C.; Ezcurra-Ciaurriz, X.; Chemisana, D.; Plà-Aragonés, L. Life Cycle Assessment (LCA) of a food-production system in Spain: Iberian ham based on an extensive system. *Sci. Total Environ.* **2022**, *808*, 151900. [CrossRef] [PubMed]

22. Notarnicola, B.; Tassielli, G.; Nicoletti, G. Life cycle assessment (LCA) of wine production. *Environ.-Friendly Food Process.* **2003**, *306*, 326.

23. Aganovic, K.; Smetana, S.; Grauwet, T.; Toepfl, S.; Mathys, A.; Van Loey, A.; Heinz, V. Pilot scale thermal and alternative pasteurization of tomato and watermelon juice: An energy comparison and life cycle assessment. *J. Clean. Prod.* **2017**, *141*, 514–525. [CrossRef]

24. Andersson, K.; Ohlsson, T.; Olsson, P. Screening life cycle assessment (LCA) of tomato ketchup: a case study. *J. Clean. Prod.* **1998**, *6*, 277–288. [CrossRef]

25. Amienyo, D.; Camilleri, C.; Azapagic, A. Environmental impacts of consumption of Australian red wine in the UK. *J. Clean. Prod.* **2014**, *72*, 110–119. [CrossRef]

26. Amienyo, D.; Azapagic, A. Life cycle environmental impacts and costs of beer production and consumption in the UK. *Int. J. Life Cycle Assess.* **2016**, *21*, 492–509. [CrossRef]

27. André, H.; Söderman, M.L.; Nordelöf, A. Resource and environmental impacts of using second-hand laptop computers: A case study of commercial reuse. *Waste Manag.* **2019**, *88*, 268–279. [CrossRef]

28. Samani, P.; van der Meer, Y. Life cycle assessment (LCA) studies on flame retardants: A systematic review. *J. Clean. Prod.* **2020**, *274*, 123259. [CrossRef]

29. Spreafico, C.; Russo, D. Exploiting the scientific literature for performing life cycle assessment about transportation. *Sustainability* **2020**, *12*, 7548. [CrossRef]

30. Jakub, S.; Adrian, L.; Mieczysław, B.; Ewelina, B.; Katarzyna, Z. Life cycle assessment study on the public transport bus fleet electrification in the context of sustainable urban development strategy. *Sci. Total Environ.* **2022**, *824*, 153872. [CrossRef]

31. Ercan, T.; Tatari, O. A hybrid life cycle assessment of public transportation buses with alternative fuel options. *Int. J. Life Cycle Assess.* **2015**, *20*, 1213–1231. [CrossRef]

32. Nordelöf, A.; Romare, M.; Tivander, J. Life cycle assessment of city buses powered by electricity, hydrogenated vegetable oil or diesel. *Transp. Res. Part D Transp. Environ.* **2019**, *75*, 211–222. [CrossRef]

33. Perčić, M.; Vladimir, N.; Fan, A. Techno-economic assessment of alternative marine fuels for inland shipping in Croatia. *Renew. Sustain. Energy Rev.* **2021**, *148*, 111363. [CrossRef]

34. Perčić, M.; Vladimir, N.; Fan, A.; Jovanović, I. Holistic Energy Efficiency and Environmental Friendliness Model for Short-Sea Vessels with Alternative Power Systems Considering Realistic Fuel Pathways and Workloads. *J. Mar. Sci. Eng.* **2022**, *10*, 613. [CrossRef]

35. Perčić, M.; Frković, L.; Pukšec, T.; Ćosić, B.; Li, O.L.; Vladimir, N. Life-cycle assessment and life-cycle cost assessment of power batteries for all-electric vessels for short-sea navigation. *Energy* **2022**, *251*, 123895. [CrossRef]

36. Park, C.; Jeong, B.; Zhou, P.; Jang, H.; Kim, S.; Jeon, H.; Nam, D.; Rashedi, A. Live-Life cycle assessment of the electric propulsion ship using solar PV. *Appl. Energy* **2022**, *309*, 118477. [CrossRef]

37. Del Pero, F.; Delogu, M.; Pierini, M. The effect of lightweighting in automotive LCA perspective: Estimation of mass-induced fuel consumption reduction for gasoline turbocharged vehicles. *J. Clean. Prod.* **2017**, *154*, 566–577. [CrossRef]

38. dos Santos Pegoretti, T.; Mathieux, F.; Evrard, D.; Brissaud, D.; de França Arruda, J.R. Use of recycled natural fibres in industrial products: A comparative LCA case study on acoustic components in the Brazilian automotive sector. *Resour. Conserv. Recycl.* **2014**, *84*, 1–14. [CrossRef]

39. Verma, S.; Dwivedi, G.; Verma, P. Life cycle assessment of electric vehicles in comparison to combustion engine vehicles: A review. *Mater. Today Proc.* **2021**, *49*, 217–222. [CrossRef]
40. Candelaresi, D.; Valente, A.; Bargiacchi, E.; Spazzafumo, G. Life cycle assessment of hybrid passenger electric vehicle. In *Hybrid Technologies for Power Generation*; Elsevier: Amsterdam, The Netherlands, 2022; pp. 475–495.
41. Vilaça, M.; Santos, G.; Oliveira, M.S.; Coelho, M.C.; Correia, G.H. Life cycle assessment of shared and private use of automated and electric vehicles on interurban mobility. *Appl. Energy* **2022**, *310*, 118589. [CrossRef]
42. Arshad, F.; Lin, J.; Manurkar, N.; Fan, E.; Ahmad, A.; Tariq, M.-u.-N.; Wu, F.; Chen, R.; Li, L. Life Cycle Assessment of Lithium-ion Batteries: A Critical Review. *Resour. Conserv. Recycl.* **2022**, *180*, 106164. [CrossRef]
43. Engels, P.; Cerdas, F.; Dettmer, T.; Frey, C.; Hentschel, J.; Herrmann, C.; Mirfabrikikar, T.; Schueler, M. Life cycle assessment of natural graphite production for lithium-ion battery anodes based on industrial primary data. *J. Clean. Prod.* **2022**, *336*, 130474. [CrossRef]
44. Zackrisson, M.; Fransson, K.; Hildenbrand, J.; Lampic, G.; O'Dwyer, C. Life cycle assessment of lithium-air battery cells. *J. Clean. Prod.* **2016**, *135*, 299–311. [CrossRef]
45. Degen, F.; Schütte, M. Life cycle assessment of the energy consumption and GHG emissions of state-of-the-art automotive battery cell production. *J. Clean. Prod.* **2022**, *330*, 129798. [CrossRef]
46. Raugei, M.; Winfield, P. Prospective LCA of the production and EoL recycling of a novel type of Li-ion battery for electric vehicles. *J. Clean. Prod.* **2019**, *213*, 926–932. [CrossRef]
47. LiBER—Lithium Battery Emilia Romagna. 2021. Available online: www.liberbattery.it (accessed on 12 June 2022).
48. Rossi, C.; Pilati, A.; Marano, M. Electric Power Module and Method for Assembling It. U.S. Patent 17/255,176, 12 August 2021.
49. Ragoni, E. L'auto Solare Emiliana che ha Conquistato l'America, Descritta da chi l'ha Progettata. *Forbes* 8 June 2018. Available online: https://forbes.it/2018/08/06/lauto-solare-emiliana-che-ha-conquistato-lamerica-descritta-da-chi-lha-progettata/ (accessed on 12 June 2022).
50. Rossi, C.; Bertoldi, M.; Fabbri, G.; Pontara, D.; Rizzoli, G. Experimental temperature modelization for solar racing vehicle. In *Sustainable Design and Manufacturing 2017, Proceedings of the International Conference on Sustainable Design and Manufacturing, Bologna, Italy, 26–28 April 2017*; Springer: Berlin, Germany, 2017; pp. 829–846.
51. Fragassa, C. Progettare e costruire un auto solare. *Il Progettista Industriale* **2015**, *2015*, 50–54.
52. Fragassa, C.; Pavlovic, A.; Minak, G. On the structural behaviour of a CFRP safety cage in a solar powered electric vehicle. *Compos. Struct.* **2020**, *252*, 112698. [CrossRef]
53. Pavlović, A.; Sintoni, D.; Minak, G.; Fragassa, C. On the modal behaviour of ultralight composite sandwich automotive panels. *Compos. Struct.* **2020**, *248*, 112523. [CrossRef]
54. Pavlovic, A.; Sintoni, D.; Fragassa, C.; Minak, G. Multi-objective design optimization of the reinforced composite roof in a solar vehicle. *Appl. Sci.* **2020**, *10*, 2665. [CrossRef]
55. Minak, G.; Brugo, T.M.; Fragassa, C. Ultra-High-Molecular-Weight Polyethylene Rods as an Effective Design Solution for the Suspensions of a Cruiser-Class Solar Vehicle. *Int. J. Polym. Sci.* **2019**, *2019*, 8317093. [CrossRef]
56. Sorrentino, S.; De Felice, A.; Grosso, P.; Minak, G. First assessment on suspension parameter optimization for a solar–powered vehicle. In *IOP Conference Series: Materials Science and Engineering*; IOP Publishing: Bristol, UK, 2019; Volume 659, p. 012080.
57. Fragassa, C.; Minak, G.; Lukovic, M.; Maglio, S. Innovation in solar vehicles: from the idea to the prototype in less than 24 months. *Eng. Sci.* **2019**, *1*, 727–730. [CrossRef]
58. Pavlovic, A.; Fragassa, C.; Minak, G.; Lukovic, M. Toward a sustainable mobility: A solar vehicle for a new quality of life. In *IOP Conference Series: Materials Science and Engineering*; IOP Publishing: Bristol, UK, 2019; Volume 659, p. 012075.
59. Melin, H.E. *Analysis of the Climate Impact of Lithium-Ion Batteries and How to Measure It*; Circular Energy Storage: London, UK, 2019.
60. Molicel®. *Safety Data Sheet*; E-One Moli Energy (Canada) Ltd.: Maple Ridge, BC, Canada, 2019.
61. *NMC Battery Material (LiNiMnCoO2)*; TARGAY: Kirkland, QC, Canada, 2022.
62. Ellingsen, L.A.W.; Majeau-Bettez, G.; Singh, B.; Srivastava, A.K.; Valøen, L.O.; Strømman, A.H. Life cycle assessment of a lithium-ion battery vehicle pack. *J. Ind. Ecol.* **2014**, *18*, 113–124. [CrossRef]
63. Encyclopaedia Britannica, T.E. *Paul-Louis-Toussaint Héroult*; Britannica: Chicago, IL, USA, 2022.
64. Kapranos, P.; Brabazon, D.; Midson, S.; Naher, S.; Haga, T. *Advanced Casting Methodologies: Inert Environment Vacuum Casting and Solidification, Die Casting, Compocasting, and Roll Casting*; Elsevier: Amsterdam, The Netherlands, 2014.
65. *Eco-Profiles for Determining Environmental Impacts of Plastics*; Plastics Europe: Brussels, Belgium, 2022.
66. Omnexus—The Material Selection Platform. *Flammability UL94—Preliminary Screening of Plastics for Fire Performance*; Boedeker Plastics, Inc.: Shiner, TX, USA, 2022.
67. Kabata; Skorek; Rajagopalan. Calculation of the direct energy consumption in heat treatment processes. In Proceedings of the Canadian Conference on Electrical and Computer Engineering, Halifax, NS, Canada, 25–28 September 1994; Volume 1, pp. 89–92
68. The Aluminum Association. *The Environmental Footprint of Semi-Finished Aluminum Products in North America*; The Aluminum Association: Arlington County, VA, USA, 2013.
69. ecoinvent Database. ei—Ecoinvent. Available online: https://ecoinvent.org/the-ecoinvent-database/ (accessed on 12 June 2022).
70. Das, S.; Liang, C.; Dunn, J.B. Life Cycle Assessment of Polymers and Their Recycling. In *Circular Economy of Polymers: Topics in Recycling Technologies*; ACS Publications: Cambridge, MA, USA, 2021; pp. 143–170.

71. von der Assen, N.; Lampe, M.; Müller, L.; Bardow, A. Life-Cycle Assessment Principles for the Integrated Product and Process Design of Polymers from CO_2. In *Computer Aided Chemical Engineering*; Elsevier: Amsterdam, The Netherlands, 2015; Volume 37, pp. 1235–1240.
72. Turbo, M.D. *Propulsion of 8000–10000 TEU Container Vessel*; MAN—MAN Energy Solutions: Augsburg, Germany, 2012.
73. *Guidelines for Measuring and Managing CO_2 Emission from Freight Transport Operations*; ECTA —European Chemical Transport Association: Schaerbeek, Belgium, 2011.
74. Life Cycle Inventory Data; CMP—Center for Environmental Assessment of Product and Material Systems. Available online: https://www.chalmers.se/en/about-chalmers/environmental-science-and-sustainable-development/Pages/center-for-environmental-assessment-of-product-and-material-systems-cpm.aspx (accessed on 12 June 2022).
75. Manjong, N.B.; Usai, L.; Burheim, O.S.; Strømman, A.H. Life Cycle Modelling of Extraction and Processing of Battery Minerals—A Parametric Approach. *Batteries* **2021**, *7*, 57. [CrossRef]
76. *Natural Resources—Brines*; SQM—Solution for Human Progress: Santiago, Chile, 2018.
77. Ambrose, H.; Kendall, A. Understanding the future of lithium: Part 2, temporally and spatially resolved life-cycle assessment modeling. *J. Ind. Ecol.* **2020**, *24*, 90–100. [CrossRef]
78. Xu, S.; Song, J.; Bi, Q.; Chen, Q.; Zhang, W.M.; Qian, Z.; Zhang, L.; Xu, S.; Tang, N.; He, T. Extraction of lithium from Chinese salt-lake brines by membranes: Design and practice. *J. Membr. Sci.* **2021**, *635*, 119441. [CrossRef]
79. External Affairs, E.D.D.M. Survey of Lithium Market—Chile. 2019. Available online: https://www.indianembassysantiago.gov.in/pdf/Survey%20on%20Lithium%20sector%20in%20Chile_compressed.pdf (accessed on 12 June 2022).
80. Stamp, A.; Lang, D.J.; Wäger, P.A. Environmental impacts of a transition toward e-mobility: the present and future role of lithium carbonate production. *J. Clean. Prod.* **2012**, *23*, 104–112. [CrossRef]
81. Jiang, S.; Zhang, L.; Li, F.; Hua, H.; Liu, X.; Yuan, Z.; Wu, H. Environmental impacts of lithium production showing the importance of primary data of upstream process in life-cycle assessment. *J. Environ. Manag.* **2020**, *262*, 110253. [CrossRef]
82. Encyclopaedia Britannica, T.E. Mineral Resources, Noncarboniferous. Britannica. Available online: https://www.britannica.com/place/Chile/Mineral-resources-noncarboniferous (accessed on 12 June 2022).
83. Chile Set to Revive Its Dormant Cobalt Sector. Resource World. 2019. Available online: https://resourceworld.com/chile-set-to-revive-its-dormant-cobalt-sector/ (accessed on 12 June 2022).
84. Majumder, R. *Chile's Export of Aluminium Foil during 2018–20 Marks a Sharp Rise with a Minimal Drop*; AICircle: Kolkata, India, 2021.
85. Ossa, A.C. Genesis of manganese deposits in northern Chile. *Econ. Geol.* **1970**, *65*, 681–689. [CrossRef]
86. Dunn, J.; James, C.; Gaines, L.; Gallagher, K.; Dai, Q.; Kelly, J.C. *Material and Energy Flows in the Production of Cathode and Anode Materials for Lithium Ion Batteries*; Argonne National Laboratory: Lemont, IL, USA, 2014.
87. *Life Cycle Assessment (LCA) of Cobalt and Cobalt Compounds*; Cobalt Institute: Guildford, UK, 2015.
88. Vega, R.A.D. Exergy Cost Assessment in Global Mining. Ph.D. Thesis, Universidad de Zaragoza, Zaragoza, Spain, 2014.
89. *Nickel Energizing Batteries*; Nickel Institute: Toronto, ON, Canada, 2021.
90. *Nickel Metal Life Cycle Data*; Nickel Institute: Toronto, ON, Canada, 2020.
91. Dai, Q.; Kelly, J.C.; Gaines, L.; Wang, M. Life cycle analysis of lithium-ion batteries for automotive applications. *Batteries* **2019**, *5*, 48. [CrossRef]
92. *Copper Environmental Profile*; International Copper Alliance: San Marcos, CA, USA, 2022.
93. NMC Powder for Battery Manufacturers. TARGAY. Available online: https://www.targray.com/li-ion-battery/cathode-materials/nmc (accessed on 12 June 2022).
94. *What Do We Know about Next-Generation NMC 811 Cathode?* Research Interfaces: Montreal, QC, Canada, 2018.
95. Ahmed, S.; Nelson, P.A.; Gallagher, K.G.; Susarla, N.; Dees, D.W. Cost and energy demand of producing nickel manganese cobalt cathode material for lithium ion batteries. *J. Power Sources* **2017**, *342*, 733–740. [CrossRef]
96. Nakanishi, S.; Suzuki, T.; Qi, C.; Akikusa, J.; Nakamura, K. Effect of surface treatment for aluminum foils on discharge properties of lithium-ion battery. *Trans. Nonferr. Met. Soc. China* **2014**, *24*, 2314–2319. [CrossRef]
97. Susarla, N.; Ahmed, S. Estimating Cost and Energy Demand in Producing Lithium Hexafluorophosphate for Li-Ion Battery Electrolyte. *Ind. Eng. Chem. Res.* **2019**, *58*, 3754–3766. [CrossRef]
98. Dunn, J.B.; Gaines, L.; Barnes, M.; Sullivan, J.L.; Wang, M. *Material and Energy Flows in the Materials Production, Assembly, and End-of-Life Stages of the Automotive Lithium-Ion Battery Life Cycle*; Technical Report; Argonne National Lab. (ANL): Argonne, IL, USA, 2014.
99. Jinasena, A.; Burheim, O.S.; Strømman, A.H. A Flexible Model for Benchmarking the Energy Usage of Automotive Lithium-Ion Battery Cell Manufacturing. *Batteries* **2021**, *7*, 14. [CrossRef]
100. Molicel® Product Data Sheet. Available online: https://www.molicel.com/products-applications/explore-by-product/ (accessed on 12 June 2022).
101. Smith, L.; Ibn-Mohammed, T.; Koh, L.; Reaney, I.M. Life cycle assessment of functional materials and devices: Opportunities, challenges, and current and future trends. *J. Am. Ceram. Soc.* **2019**, *102*, 7037–7064. [CrossRef]
102. Silicon-Chemistry Carbon Balance—An assessment gas emissions and reductions. CES—Silicones Europe. Available online: https://www.silicones.eu/wp-content/uploads/2019/05/SIL_exec-summary_en.pdf (accessed on 12 June 2022).
103. The World's Leading, High Performance, Open Source Life Cycle Assessment Software. openLCA. Available online: https://www.openlca.org/ (accessed on 12 June 2022).

104. Senatore, V.; Buonerba, A.; Zarra, T.; Oliva, G.; Belgiorno, V.; Boguniewicz-Zablocka, J.; Naddeo, V. Innovative membrane photobioreactor for sustainable CO_2 capture and utilization. *Chemosphere* **2021**, *273*, 129682. [CrossRef]
105. Song, Y.S.; Youn, J.R.; Gutowski, T.G. Life cycle energy analysis of fiber-reinforced composites. *Compos. Part A Appl. Sci. Manuf.* **2009**, *40*, 1257–1265. [CrossRef]
106. Yang, Y.; Boom, R.; Irion, B.; van Heerden, D.J.; Kuiper, P.; de Wit, H. Recycling of composite materials. *Chem. Eng. Process. Process. Intensif.* **2012**, *51*, 53–68. [CrossRef]
107. Giorgini, L.; Benelli, T.; Brancolini, G.; Mazzocchetti, L. Recycling of carbon fiber reinforced composite waste to close their life cycle in a cradle-to-cradle approach. *Curr. Opin. Green Sustain. Chem.* **2020**, *26*, 100368. [CrossRef]